# On the Thermonuclear Runaway in Type Ia Supernovae:

# How to run away?

P. Höflich

<sup>1</sup>Department of Astronomy, University of Texas, Austin, USA
pah@hej1.as.utexas.edu

J. Stein

<sup>2</sup> Racah Institute of Physics, The Hebrew University of Jerusalem, Israel
yossi@phys.huji.ac.il

#### ABSTRACT

Type Ia Supernovae are thought to be thermonuclear explosions of massive white dwarfs (WD). We present the first study of multi-dimensional effects during the final hours prior to the thermonuclear runaway which leads to the explosion. The calculations utilize an implicit. 2-D hydrodynamical code. Mixing and the ignition process are studied in detail. We find that the initial chemical structure of the WD is changed, but the material is not fully homogenized. In particular, the exploding WD sustains a central region with a low C/O ratio. This implies that the explosive nuclear burning will begin in a partially carbon-depleted environment. The thermonuclear runaway happens in a well-defined region close to the center. It is induced by compressional heat when matter is brought inwards by convective flows. We find no evidence for multiple spot or strong off-center ignition. Convective velocities in the WD are of the order of 100 km/sec which is well above the effective burning speeds in SNe Ia previously expected right after the runaway. In our calculations, the ignition occurs near the center. Then, for  $\approx$ 0.5 to 1 sec, the speed of the burning front will neither be determined by the laminar speed nor the Rayleigh-Taylor instabilities but by convective flows produced prior to the runaway. The consequences are discussed for our understanding of the detailed physics of the flame propagation, the deflagration to detonation transition, and the nucleosynthesis in the central layers. Our results strongly suggest the pre-conditioning of the progenitor as a key factor for our understanding of the diversity in Type Ia Supernovae.

 $Subject\ headings:$  supernovae - white dwarfs - hydrodynamics - convection

# 1. Introduction

Type Ia Supernovae (SNe Ia) are among the most spectacular events because they reach the same brightness as an entire galaxy. This makes them good candidates to determine extragalactic distances and to measure the basic cosmological parameters. Moreover, they are thought to be the major contributors to the chemical enrichment of the interstellar matter with heavy elements. Energy injection by SN into the interstellar medium, triggered star formation and feedback in galaxy formation are regarded as a key for our understanding of the formation and evolution of galaxies.

There is general agreement that SNe Ia result from some process of combustion of a degenerate, C/O white dwarf (Hoyle & Fowler 1960). Within this general picture, three classes of models have been considered: (1) An explosion of a CO-WD, with mass close to the Chandrasekhar mass, which accretes mass through Roche-lobe overflow from an evolved companion star (Whelan & Iben 1973). The explosion is then triggered by compressional heating near the WD center. (2) An explosion of a rotating configuration formed from the merging of two low-mass WDs, caused by the loss of angular momentum due to gravitational radiation (Webbink 1984, Iben & Tutukov 1984, Paczyński 1985). (3) Explosion of a low mass CO-WD triggered by the detonation of a helium layer (Nomoto 1980, Woosley et al. 1980, Woosley & Weaver 1986). Only the first two models appear to be viable. The third, the sub-Chandrasekhar WD model, has been ruled out on the basis of predicted light curves and spectra (Höflich et al. 1996a, Nugent et al. 1997).

For the identification of the most common scenario, the main problem is related to the insensitivity of the WD structure to the progenitor star and system. However, the last decade has witnessed an explosive growth of high-quality data and advances in the models for supernovae which opened up new opportunities to constrain the physics of supernovae. For the first time, a direct connection with the progenitors seems to be within reach. In particular, there is mounting evidence for a connection between the properties of the progenitor, and the physics of the explosion.

The explosion of a WD with  $M_{Ch}$  is the most likely candidate for the majority of 'normal' SNe Ia. In particular, delayed detonation (DD) models (Khokhlov 1991, Woosley & Weaver 1994, Yamaoka et al. 1992) have been found to reproduce the majority of optical and infrared light curves (LC) and spectra of SNe Ia reasonably well (Höflich 1995; Höflich & Khokhlov 1996; Fisher et al. 1998; Nugent et al. 1997; Wheeler et al. 1998; Lentz et al. 2000; Gerardy et al. 2001). We note that detailed analyzes of observed spectra and light curves indicate that mergers and deflagration models such as W7 may contribute to the supernovae population (Harkness 1987, Höflich & Khokhlov 1996, Hatano et al. 2000). The evidence against pure deflagration models for the majority of SNeIa includes IR-spectra which show signs of explosive carbon burning at high expansion velocities (e.g. Wheeler et al. 1998) and recent calculations for 3-D deflagration fronts by Khokhlov (2001) which predict the presence of unburned and partially burned material down to the central regions, and a large amount of unburned material at the outer layers. Mergers are beyond the scope of this paper but pure deflagration models will be mentioned where appropriate.

The DD-model assumes that burning starts as subsonic deflagration and then turns to a supersonic, detonative mode of burning. The amount of  $^{56}$ Ni depends primarily on  $\rho_{tr}$  (Höflich 1995; Höflich; Khokhlov & Wheeler 1995; Iwamoto et al. 1999), and to a much lesser extent on the deflagration speed, and the initial central density and initial chemical composition (ratio of carbon to oxygen) of the WD. In DDs, almost the entire WD is burned, i.e. the total production of nuclear energy is almost constant. This and the dominance of  $\rho_{tr}$  for the  $^{56}Ni$  production are the basis of why, to first approximation, SNe Ia appear to be a one-parameter family. The observed  $M(\Delta M_{15})$  can be well understood as an opacity effect, namely the dropping opacity at low temperatures (Höflich et al. 1996b and references therein; Mazzali et al. 2001). Nonetheless, variations of the other parameters lead to some deviation from a one-parameter  $M(\Delta M_{15})$  relation with a spread of  $0.5^m$  (Höflich et al. 1996b). Empirically, the  $M(\Delta M_{15})$  has been well established with a rather small statistical error  $\sigma$  (0.12 $^m$ : Riess et al. 1996; 0.16 $^m$ : Schmidt et al. (1998); 0.14 $^m$ : Phillips 1999; 0.16 $^m$ : Riess et al. 1999; 0.17 $^m$ : Perlmutter et al. 1999a). This may imply a correlation between free model parameters, namely the properties of the burning front, the main sequence mass of the progenitor  $M_{MS}$ , and the central density of the WD at the time of the explosion.

Recent studies have shown that the chemical structure of the WD will affect the LCs and spectra. The properties of the progenitors must be taken into account to determine cosmological parameters or the cosmological equation of state. In particular, the mean C/O ratio of the exploding WD has been identified as one of the key factors (Höflich et al. 1998, 2000; Umeda et al. 2000; Dominguez, Höflich & Straniero 2001). From stellar evolution, the WD can be expected to consist of a C-depleted central region produced during the convective, central He burning. The central region is surrounded by layers with  $C/O \approx 1$  originating from the He-shell burning in the star and from the accretion phase. The size of the C-depleted region ranges from 0.1 to about 0.8  $M_{\odot}$  depending on  $M_{MS}$ . At the time of the explosion, the C/O-WD should show a distinct C and O profile, These dependencies may suggest that the pre-conditioning of the WD may be key for our understanding of the diversity of supernovae (Höflich et al. 1996). In addition, Arnett & Livne (1994) suggested that the initial velocity fields in the WD prior to the explosion might influence the flame propagation.

The propagation of a detonation front is well understood but the description of the deflagration front and the deflagration to detonation transition (DDT) pose problems. On a microscopic scale, a deflagration propagates due to heat conduction by electrons. Though the laminar flame speed in SNe Ia is well known, the front has been found to be Rayleigh-Taylor (RT) unstable, increasing the effective speed of the burning front (Nomoto et al. 1976). More recently, significant progress has been made toward a better understanding of the physics of flames. Starting from static WDs, hydrodynamic calculations of the deflagration fronts have been performed in 2-D (Niemeyer & Hillebrandt 1995, Reinecke et al. 1999, Lieswski et al. 2000) and 3-D (e.g. Livne 1993, Khokhlov 1995, Khokhlov 2001). It has been demonstrated that R-T instabilities govern the morphology of the burning front in the regime of linear instabilities, i.e. as long as perturbations remain small. During the first second after the runaway, the increase of the flame surface due to RT remains small and the effective burning speed is close to the laminar speed ( $\approx 50 km/sec$ ) if the ignition occurs close to the center. Khokhlov (2001) also shows that the effective burning speed is very sensitive to the energy release by the fuel, i.e. the local C/O ratio. Therefore, the actual flame propagation will depend on the detailed chemical structure of the progenitor. Niemeyer, Hillebrandt & Woosley (1996) studied the effect of off-center ignition and demonstrated that multiple-spot ignition with significant separation ( $\approx 50...100km$ ) will significantly alter the early propagation of the flame. For strong off-center ignitions, the buildup time of RT-instabilities is shorter corresponding to the larger gravitational acceleration. Still, even for fast rising blobs, their morphology and, consequently, the effective burning speed will depend critically on small scale motions of the background (see below).

Despite these advances, the mechanism is not well understood which leads to a DDT or, alternatively, to a fast deflagration in the non-linear regime of instabilities. Possible candidates for the mechanism are, among others, the Zeldovich mechanism, i.e. mixing of burned and unburned material (Khokhlov, Oran & Wheeler 1997ab, Niemeyer & Woosley 1997), crossing shock waves produced in the highly turbulent medium, or shear flows of rising bubbles at low densities (Livne, 1998). Currently, none of the proposed mechanisms have been shown to work in the environment of SNe Ia. The Zeldovich mechanism leads to a DDT only if the density and temperature fluctuations remain small (Niemeyer 1999), and the effectiveness of crossing shock waves or shear flows has yet to be demonstrated. However, as a common factor, all these mechanism will depends on on the physical conditions prior to the DDT.

From the analysis of LCs and spectra, and the study of flame fronts in SNe Ia, there are strong indications for the importance of the initial structure of the WD prior to the nuclear runaway.

In this work we present the evolution of the WD just prior to the thermonuclear runaway based on multidimensional calculations. In particular, we want to address the following questions: 1) Do mixing processes change the chemical structure of the WD prior to the explosion? 2) Does the thermonuclear runaway occur in multiple spots? 3) Does the thermonuclear runaway happen in a static white dwarf? In Section 2 we present the setup of our calculations. In Section 3, the results are presented. In the final, concluding section, we discuss the results in the context of the modeling of SNe Ia, the use of SNe Ia as cosmological yard sticks, and address the limits of our study.

# 2. Numerical Methods and Setup

The initial model has been constructed from results for the stellar progenitor evolution based on the code FRANEC (Straniero et al. 1988, Chieffi et al. 1989, Limogni et al. 2000). The subsequent accretion phase on the WD has been followed up to the thermonuclear runaway by solving the standard equations for stellar evolution in a Henyey scheme (Höflich et al. 2000). Nomoto's equation of state is used (Nomoto et al. 1982). For the energy transport, conduction (Itoh et al. 1983), convection in the mixing length theory, and radiation are taken into account. Radiative opacities for free-free and bound-free transitions are treated in Kramer's approximation and by free electrons. A nuclear network of 35 species up to  $^{24}Mg$  is taken into account based on the reaction network of Thielemann, Nomoto & Hashimoto (1996).

For our study of multidimensional effects, we start from a WD model several hours before runaway. The spherical model is re-mapped on a spherical grid with 191 radial and 31 angular  $(\Theta)$  zones within a cone with  $\Theta$  between 45° and 135°. The radial resolution has been decreased by a factor of  $\approx 10$  from inner to the outer layer to properly resolve the central regions. Note that the effective Reynolds numbers are of the order of 30 in the convective region. Thus, we cannot resolve the small scale, turbulent motion but our study is limited to the large scale, convective flows. The initial structure is relaxed on this grid assuming a pure carbon/oxygen mixture. To carry out multi-dimensional simulations of the interior convection; and because of the low Mach number of the associated flows, a compressible implicit hydro code is required. For available explicit, compressible codes for thermonuclear burning, the sound crossing time over a resolution element limits the time step, i.e. CFL condition which imposes hopelessly short time steps. Therefore, for the further evolution, we use an implicit, Eulerian 2-D hydrodynamical code (Stein, Barkat & Wheeler 2001). The perpendicular velocity is assumed to be zero [reflective] at all boundaries. The hydrodynamical equations are solved in a  $2^{nd}$  order scheme including first order centrifugal and Coriolis forces. Radiation transport effects have been neglected. For the equation of state, we use a relativistic Fermi-gas with Coulomb corrections, and radiation. Nuclei are treated as an ideal, non-relativistic gas without crystallization. For the nuclear burning, analytic expressions have been used for the production of nuclear energy (Rakavy & Shaviv 1968, Barkat et al. 1990), and calibrated by an  $\alpha$ -network and tested against the detailed network given above (Thielemann et al. 1996). The time step has been limited by the flow of the material from zone to zone. Typically, the maximum exchange of matter is limited to  $\approx 5\%$ . We use standard quadratic artificial viscosity, and small second-order Lax throughout the star. Small first order Lax is used in the inner 3 rows of cells, and in the outer cells. Small scale fluctuations were introduced to initialize the convection. Tests showed that the results do no depend on the initial spectrum of the fluctuations.

#### 3. Results

The structure of the initial model of the C/O white dwarf is based on a star with 3 solar masses at the main sequence and solar metallicity which, at the end of its evolution, has lost all of its H and He-rich layers. By accretion, its core has been grown close to the Chandrasekhar limit (Dominguez et al. 1998, Dominguez & Höflich 2001). The temperature, density and chemical profile at about 1 day before runaway (in 1-D) have been re-mapped to the 2-D grid. At this time, the central density of the WD is  $2 \times 10^9 g/cm^3$ . The carbon concentration in the inner layers with 0.348  $M_{\odot}$  is a result of the central helium burning during the stellar evolution. For the outer layers, the C/O ratio is close to 1. At this time, the nuclear burning times scales are of the order of days, i.e. much longer than the hydrodynamical time scales ( $\approx 1sec$ ). Because the WD is almost isothermal, the entropy is increasing with radius. The initial structure is shown in Fig.1 (after relaxation). In the reference model, the further evolution has been followed up all the way to the thermonuclear runaway. The computational domain extends between 65 km to 2000 km in the radial direction. For the detailed study of the runaway, we use an extended computational domain down to 13.7 km.

#### 3.1. Evolution of the Reference Model

#### 3.1.1. The Mixing Phase

The nuclear time scales are long compared to the hydrodynamical time scales up to a few seconds before runaway. Because most of the mixing of abundances happens during this stage of long nuclear time scales (see below), it will be referred to as 'mixing phase'.

In Figs. 2, 3 & 4, snapshots of the evolution are shown for various quantities at 2 and 1 hours, 15 and 5 minutes before the runaway. Nuclear burning of  $^{12}C$  in the central region increase the entropy and temperature. Consequently, the rate of energy production grows with time. The increase of temperature by about 24 % in the central regions results in a decrease of the central density by about 4 %. Most of the nuclear energy contributes directly to an increase of the entropy. In addition, the nuclear burning drives large scale, convective flows. Typical velocities of the convective flows increase from about 10 km/sec at 2 hours before runaway (b.r.) to  $\approx 50 km/sec$  at about 5 minutes b.r. (Fig. 4 and see below). The size of the eddies is comparable to the pressure scale height ( $\approx 100km$ ) (see Fig. 2). The life time of individual eddies is of the order of one revolution for a mass element, leaving little chance to produce a pattern typical for stationary convective layers. The flow is statistically steady on time scales short compared to the nuclear evolution time scales up to about 1 hour before the runaway. Eventually, most of the kinetic energy dissipates and contributes to heating. At the time of the explosion, the kinetic energy is small compared to the nuclear energy produced (7.01<sup>45</sup> vs. 2.456<sup>48</sup> erg). Initially, the convective region is confined by the chemical boundary. Later on, the entropy grows inside by nuclear burning, and a core of almost constant entropy forms. The convection is confined by the steep entropy gradient as a consequence of the steep entropy rise in the outer layers (caused by the flat temperature profile in combination with the rapidly decreasing density, see above). Due to the increase of the entropy with time, this boundary is gradually moving outwards in both mass and radius. Consequently, material of the carbon rich mantel and the core are mixed. The carbon concentration in the center increases from 24.7 to 35.6 % at the time of the runaway and its size grows from 540 to 730 km (Fig. 5). Due to the small energy production, hardly any mixing occurs early on but the rate of mixing and of the change of R, i.e. the contour with C=45\%, grows strongly with time as the nuclear burning increases. No evidence is found for rising blobs which pass the

sharp boundary of convective and non-convective layers and stay there. Blobs which pass the boundary tear pieces from the non-convective layer, creating a new sharp boundary. In stellar evolution, penetration of individual elements of about 0.2 to 0.25 pressure scale heights is assumed by some authors (e.g. Bressan et al. 1993, Schaller et al. 1992). If present, this effect would result in a chemical mixing of the entire WD with time scale of a few hours. In our example, a significant fraction of the WD mass is enclosed within about 3 scale heights above the chemical inhomogeneity which corresponds to a distance of 500 km. If we assume h=0.25 and a velocity of 10 km/sec for the turbulent eddies, the corresponding time scale for complete mixing would be  $\approx 3h$ .

For any given progenitor structure, the lack of passing blobs through the boundary of convective and non-convective region allows us to estimate the total amount of mixing even without detailed calculations. During the phase of slow burning, only a negligible fraction of the C is consumed, the turbulent region is confined by the steep entropy gradient at the chemical boundary, and the entropy is almost constant within the turbulent center (Fig. 6). Nuclear runaway occurs in our model when the mean entropy in the core increases to  $\approx 10.4$ . Nuclear burning increases the level of entropy in the core. We can estimate the final amount of mixing and the radius of the core by identifying the distance in the initial model at which the entropy correspond to the critical value for the runaway. Our estimate hardly depends on the exact value of the entropy at the runaway due to the steepness of the entropy gradients.

### 3.1.2. The Nuclear Runaway: The Last 5 Minutes before Runaway

In Fig. 7, we show the final evolution of the temperature and the velocities. Increasing nuclear burning in the inner 100 km drives increasingly strong convection. The region of enhanced energy production heats up material. This hot material starts to rise. Typical turbulent velocities increase from  $\approx 50$  to  $\approx 100 km/sec$  at the time of the runaway.

The unsteady convective flows are a key factor to understand the trigger for the final thermodynamical runaway. It explains why we do not see ignition in multiple spots or a strong 'off-center' ignition. Due to convective mixing, the entropy remains nearly constant in all but the very inner layers with a central distance  $\leq 150 km$ . There, large scale, convective motion brings in material radially. Eventually, compressional heat causes the thermonuclear runaway close to the minimum distance of the corresponding eddy. In the reference model, the thermonuclear runaway occurs very close to the inner boundaries at a distance of 65km in one specific cell. In general, we do not expect multiple spot ignition because the size of the eddies is larger than the central distance of the point where the runaway occurs. We note that the convection also operates at larger distances from the center but, there, the relative changes in radius and, therefore, the release of compressional heat is insufficient to bring material to the point of explosive nuclear burning. We expect that the thermonuclear runaway occurs earlier than in 1-D models in which it is triggered by the overall compression of the WD.

To study the thermonuclear runaway in more detail, we have recalculated the final stages up to the runaway for the same model, but the computational region has been extended down to 13.7 km. For computational efficiency, we started with an increased rate of nuclear reactions by factors of 200 down to 4 up to about 10 minutes and 127 seconds before the explosion, respectively. At 127 seconds, the resulting structure resembles very closely the reference model for the entropy, the density and the chemical structure because the main effect of the nuclear burning is an increase of the entropy, the resulting mixing, and the short life time of convective cells (see sects. 3.1.1 and 3.1.3). However, the increased heating results in a

slight increase of the total kinetic energy at t=127 sec by about 10 % compared to the reference model. Fig. 9 shows the final structure at the onset of the thermonuclear runaway for the inner 120 km. Any deviations from a radial structure are limited to this inner region. Eventually, the thermonuclear runaway occurs in one cell at about a distance of 27 km. During this last phase, the strong release of nuclear energy drives large scale of violent motion of the matter. The pattern in the temperature and energy release follows the large scale motion. Most noticeable is the C-like pattern of the temperature distribution close to the center (Fig. 9, lower left panel). The density shows only very minor deviations from sphericity. At this stage of evolution, Carbon is locally depleted by about 1 to 2 % due to the nuclear burning and, again, it is carried by the velocity field.

We want to discuss the evolution to the thermonuclear runaway in some detail. As shown above, the structure of the entropy, temperature, nuclear energy production and chemistry can by understood in the same way as a result of the convective motion. As an example, the evolution of the temperature and the velocity field is shown in Fig. 8. In the following, the coordinates in brackets provide the coordinates of features in the (x,y) plane in km. At about 3.54 seconds (fig. 8, left upper plot) before the runaway, the temperature structure starts to deviate from the radial structure. The high velocity field at the upper part of the plot (red arrows) is part of a larger vortex A with the center at (150km,-10km) which extends down to about 70 km. Close to the center of the WD, nuclear burning drives a convective flow in the opposite direction. These two regions are separated by a layer with higher temperature and low velocities. Due to the shear, a new, small vortex B is evolving at (-15km,+65km). It results in a redirection of the material flow at the lower edge of vortex A. This material flow is directed inwards, and compresses and heats up material in front of the flow pattern. At about 0.353 seconds, the temperature has risen up to  $8.5 \times 10^8 K$ . Eventually, further compression and burning causes a rise in temperature up to the onset of explosive carbon burning ( $\approx T \geq 1.3 \times 10^9 K$ ).

Previously, Garcia-Senz & Woosley (1994) studied the details of the thermonuclear runaway in 1-D. They considered plumes rising in a static background. They found that the runaway occurs in rising plumes which rise with velocities of about 5 to 30 km/sec at central distances of 30 and 100 km/sec, respectively. The runaway occurred when the increase in the thermonuclear burning in the plume becomes stronger than the cooling by expansion. In our simulations, we similarly see that plumes with increased burning tend to rise close to the thermonuclear runaway. In our calculations, these plumes form close to the central region ( $\leq 30...60km$ ) due to the temperature increase close to the center. At times close to the runaway, the nuclear energy production in the plumes almost compensates for the cooling. However, in a moving background (with velocities  $\leq 100km/sec$ ), the rising plume will be disrupted and parts find themselves in both a rising and descending velocity fields. For those parts that go downward by the current, adiabatic expansion will not avoid the runaway but, in contrast, compression will push the element over the 'edge'. In a non-stationary WD, the thermonuclear runaway will occur slightly earlier than in a static WD.

## 3.1.3. Effects of the Nuclear Reaction Rates

We have studied the sensitivity of our results to the assumptions and uncertainties related to the nuclear energy production. In particular, the reaction  $^{12}C(\alpha,\gamma)^{16}O$  must be regarded as uncertain by a factor of three (e.g. Buchmann, 1997) despite some indirect evidence which favors a large cross-section. This indirect evidence stems from recent studies of pulsating WDs (Metcalfe, Winget & Nather 2001) and from the rise times of light curves of SNe Ia (Höflich et al. 1998, Dominguez et al. 2001). Stellar evolution for the asymptotic giant branch favors also a high cross section for  $^{12}C(\alpha,\gamma)^{16}O$ , but a low value can be

compensated for by an increased mixing of helium into the stellar core (e.g. Salaris et al. 1993).

We have scaled the rate for the nuclear energy production by factors f between 1 and 200 (Table 3.2). For the same initial model, a higher production of nuclear energy drives a faster convection (see  $E_{kin}$  in Tab. 1), and it decreases the time till the thermonuclear runaway, i.e. the nuclear burning time scales are reduced by the factor f. This leaves less time for mixing coupled with increased fluctuations of the central carbon abundance, so a large f implies that a lower compression is required to trigger the explosion. In all calculations, single spot ignition has been found. However, the central distance of the thermonuclear explosion increases from 27 km (f = 1) to about 90 km (f = 200), and the typical, convective velocities increase slightly. The fluctuations in the carbon concentration rise from the 1 % level to about 5 %. The amount of carbon mixing decreases with an increasing reaction rate but, overall, it is rather insensitive for  $f \leq 20$  (Fig. 10).

#### 3.2. Final Discussions and Conclusions

We have studied the final hours of a Chandrasekhar-mass WD prior to the thermonuclear runaway to investigate the pre-conditioning of exploding WDs, namely chemical mixing and the ignition process.

The initial model has been constructed from results of stellar evolution for a star with 3 solar masses with solar metallicity, followed by a subsequent accretion phase close to the onset of the thermonuclear runaway (Dominguez et al. 2001). The WD has a mass of  $\approx 1.37 M_{\odot}$ . Its chemical structure is characterized by a central region of  $0.348 M_{\odot}$  with a low C-concentration ( $\approx 24\%$ ) surrounded by a mantel with  $C/O \approx 1$  originating from the He-shell burning and the phase of accretion. A few hours before runaway, the thermal structure of the progenitor shows a rather flat temperature profile, and a steep entropy profile because the rapidly dropping density.

Prior to the runaway, the central regions undergo mild C-burning. The resulting energy release drives convective motion in the inner region of low C-concentration and, gradually, increases the entropy of the core up to the point of ignition. Due to the convection, the entropy of the core is almost constant. Within the resolution of our models, the carbon-concentration gradient at the boundary between the core and the mantle prevents direct mixing, e.g. due to overshooting convective elements. However, the increasing entropy of the core results in a negative entropy gradient at the core boundary which compensates for the carbon-concentration gradient. This increases the region with constant entropy and produces mixing of C-rich region into the core with typical fluctuation of about 1%. We find that the central C-abundance increases from 24 to about 37%. The initial WD is not homogenized, but the jump in the carbon abundance is reduced by a factor of  $\approx 2$ .

At the time of the explosion, a pattern of large scale, convective elements has been established with sizes of typically 100 km and convective velocities between  $\approx 40$  to  $\approx 120$  km/sec. Differential velocities between adjoining eddies are larger by a factor of 2 which is well in excess of the laminar deflagration speed. Thus, the change of the morphology of the burning front of SNe Ia is determined by the pre-conditioning of the WD during the early phase of the explosion for  $\approx 0.5$  to 1 sec (Dominguez & Höflich 2000, Khokhlov 2001). Niemeyer et al. (1996) found significantly shorter time scales for the growth of RT-instabilities in their study of strongly off-center explosions. This can be expected as a result of the larger gravitational acceleration. Still, even for their fast rising, large scale blobs ( $\approx 1000 km/sec$ ), the morphology of the plumes and, consequently, the effective burning speed will depend critically on small scale motions of the background. The effective surface of the front will be increased resulting in significantly higher burning

speeds. Faster burning implies a larger region of low proton to nucleon ratio and, thus, a larger production of neutron rich isotopes in the central region. On the other hand, a reduction of the time scales for electron capture can be expected leading to the production of less neutron rich isotopes. Possible consequences for current estimates on the limits on the central densities of the WD should be noted (Brachwitz et al. 2000).

The explosive nuclear burning front starts in one well defined region close to the center ( $\approx 30km$ ). The size of the ignition region is determined by the grid resolution ( $\approx 2km$ ). The explosive phase of burning is triggered by compressional heat when matter is brought inwards by convection. It starts close to the center because, there, the adiabatic heating combined with thermonuclear reactions are most effective for a given size of turbulent elements. We find no evidence for multiple spot or strong off-center ignition. We do not expect it because the size of the eddies is comparable to the central distance of the ignition point, and the lack of any mechanism which would cause a synchronization within typical time scales for the runaway ( $\leq 0.1sec$ ). Thus, the probability is fairly small for having a second ignition point during that time.

In the following, we want to put our basic results into context for our understanding and the quantitative modeling of SNe Ia. As mentioned in the introduction, the propagation of the deflagration front depends on the energy release and, consequently on the fuel (Khokhlov 2001). We find that the chemical profile in the WD will be strongly changed, but in a predictable way. We find that the initial velocity field must be expected to alter the flame propagation during the deflagration phase. Although the actual deflagration speed has little effect on the overall chemical structure of DD-models with the exception of the production of neutron rich isotopes close to the center, all proposed mechanisms for the DDT identify the pre-conditioning of the material during the deflagration phase as a key element (see introduction) which, in turn, is strongly effected by the initial WD.

We may suspect from the comparison between normal bright and subluminous SNe Ia and the role of the DDT transition for the brightness decline relation that the precondition of the WD may be the 'smoking gun' for our understanding of the diversity of SNe Ia.

As mentioned above, the overall chemical structure of the initial WD is preserved, and the turbulent velocity field is limited to the inner, C-depleted core. Both the velocity field and the C-concentration influence the burning front. Therefore, the mass of the progenitor has a direct influence on the outcome because the core size depends mainly on the  $M_{MS}$  mass of the progenitor. The consequences are obvious with respect to the evolution of the SNe Ia with redshift and their use as a yardstick to measure cosmological parameters and the cosmological equation of state.

Finally, we have also to mention the limitations. This study should not be seen as a final answer but as a starting point to open a new path which, eventually, may lead to a deeper understanding of the relation between the progenitor and the final thermonuclear explosion.

This work is based on hydrodynamical simulations in two rather than three dimensions. In either case, the convection is driven by entropy gradients over large distances. These large gradients drive large eddies. Convective eddies lose energy both in the true 3-D case and in our 2-D simulations mostly by exchange with eddies of different size but the mechanism and rate of energy loss differ between 2-D and 3-D (see below). Interaction between eddies of different sizes causes exchange of energy towards larger and smaller eddies (Porter & Woodward 1994).

It is well known that, for a fully developed turbulence in an incompressible fluid, the direction of the average energy flow is from large scale eddies to smaller ones in 3-D, and from small scale eddies to larger ones in 2-D (Kraichnan 1967, Rose & Sulem 1978, Kraichnan & Montgomery 1980). The viscosity of the

fluid becomes most important and, thus, the dissipation of kinetic energy is most efficient for the smallest eddies whose Reynolds number is comparably with unity (Laundau & Lifshitz 1989). For incompressible fluids, the dissipation of kinetic energy is very different in 2-D and 3-D. In the limiting case of vanishing viscosity and incompressible fluids, the dissipation rate in 3-D remains finite while it approaches zero in 2-D because the inverse cascade in the energy flow. The different behavior of the average energy flow in 2-D and 3-D is caused by quadratic invariants globally conserved by the advection term in the hydro equations (see e.g. Hasegawa 1985 and, more general, Vazquez-Semadeni 1991). These quantities are not conserved in compressible fluids where the difference between 2-D and 3-D will be of a different kind. Namely, energy can dissipate by acoustic waves and shocks, in addition to the energy dissipation by viscosity. Thus, the interaction of the largest eddies in a finite space and in case of a compressible fluid is less clear.

In our simulations, the decay time scales of large eddies are of the order of one rotation. The real viscosity of astrophysical fluids is much smaller than the numerical viscosity in our simulations. At the same time, large scale flows (rolls) have a higher inertia in 2-D than in 3-D. We do not know whether the lifetimes of the true large 3-D eddies are larger or smaller than in our simulations but we argue that the decay times of one rotation may be the right order of magnitude. In the following paragraphs, we argue that the main results hold. No detailed simulations for 3-D are available for the conditions in Chandrasekhar mass WDs and subsonic convection. However, 3-D studies and simulations for convection in other environments suggest dissipation time scales very similar to our results. For incompressible fluids, the dimensional analysis suggests decay time scales of the order of the revolution time in the largest eddies (Landau & Lifshitz, 1989). For fully compressible thermal convection in deep atmospheres, Porter & Woodward (2000) extended their 2-D to 3-D, and found similar results in both cases. Recent simulations for the supersonic case and MHD turbulence by Stone, Ostriker & Gammie (1998) indicate typical time scales for the energy dissipation in molecular clouds of about 0.3 to 0.8 revolutions for large eddies, i.e. about 1.5 times faster compared to similar, 2-D calculations by Ostriker, Gammie & Stone (1999).

A further restriction is our resolution which is limited to Reynolds numbers of  $\approx 30$  to 50, i.e. not sufficient to follow the cascades to small scales. Obviously, a high resolution, full three dimensional study would be desirable. In spite of this, we expect no qualitative change of our basic conclusions concerning the mixing and ignition process.

It is well known that the mixing properties of 2-D and 3-D unsteady flows differ, both for scalar and vector "contaminants". In 2-D, each large eddy is a huge torus carrying a mass which is a large portion of the convection zone, and one or two large eddies carry the hot material from the burning center and spread it over the convective zone. In 3-D, each large eddy carries much less mass. Nevertheless, even in 3-D, the number of large eddies should be sufficient for spreading material over the entire convective zone because mixing continues for hours compared to the few seconds it takes a mass element to cross the convection zone. As mentioned in the last section, the amount of mixing can be understood in terms of the nuclear burning which increases the entropy in the central region both in 2-D and 3-D calculations and, therefore, we expect a similar amount of mixing in both cases despite the differences in the mixing properties. Though, one may expect some change in the size of the fluctuations in the C-abundance and entropy (see above).

We do not expect a qualitative change in size of the large eddies at the time of runaway and, therefore, in the ignition process, because the presence of large eddies is determined by their production. The motion is continuously driven by nuclear burning at the innermost layers which produces a rise of heated material over about a pressure scale height. This determines the size of the largest eddies which must be expected to be of similar size in both 2-D and 3-D. Close to the thermonuclear runaway, the circulation times become larger than the nuclear burning time scales. Unless, in 3-D, the decay times of large eddies are much shorter

than a revolution, the largest eddies must be expected to trigger the ignition in a way similar to the 2-D case. Therefore, the probability of ignition in more than one well defined region remains small. Due to the resolution of our simulation, this region has a size of several kilometers. We cannot say anything about the ignition process on scales of the nuclear burning front.

We have discussed possible implications for the deflagration front on SNe Ia based on previous studies. Obviously, there is a need for consistent calculations of the deflagration front to quantify our estimates on the propagation of the nuclear flames.

Our results are based on a specific progenitor with a main sequence mass of  $3 M_{\odot}$ . Similar studies may be useful for other  $M_{MS}$  with larger or smaller cores with low carbon abundances, and different central densities at the time of the explosion. In light of the analysis of the subluminous SN1999by (Howell et al. 2001), other effects such as rotation or crystallization should be considered in the future.

#### ACKNOWLEDGMENTS

We would like to thank Z. Barkat, A. Glasner, A. Khokhlov, E. Livne, J. Scalo and J.C. Wheeler for helpful discussions and useful comments, and R. Hix for providing the calibration of the analytic energy production rates. J. Stein would like to thank J.C. Wheeler and the colleagues at the Department for Astronomy for the hospitality during his sabbatical in 1995-6 when this work was started, and during subsequent visits in 1997-2000. P.H. would like to thank the colleagues at the Racah Institute in Jerusalem for the hospitality during his visit. This research was supported in part by NASA Grant LSTA-98-022, and the John W. Cox Endowment Fund to the Department of Astronomy at UT.

### REFERENCES

Arnett D., Livne E. 1994, ApJ 427, 330

Barkat Z., Livne E., Swartz D.A., Wheeler J.C. 1990, in: Supernovae, Jerusalem Winter School for Theoretical Physics 88/89, Vol. 6, p. 141

Bressan A., Fagotto F. Bertelli D., Chiosi C. 1993, A&AS 100, 647

Brachwitz F., Dean, D. J., Hix R., Iwamoto K., Langanke K., Martnez-Pinedo G., Nomoto K., Strayer M., Thielemann F.K., Umeda, H. 2000, ApJ 536, 934

Buchmann L. 1997, ApJ 479, L153

Chieffi, A., and Straniero, O. 1989, ApJS, 71, 48

Caughlan G.R , Fowler A.M. 1985, ARA&A, 21, 165

Dominguez I., Höflich P., Straniero O. 2001, ApJ, submitted

Dominguez I., Höflich P. 2000, ApJ 528, 854

Dominguez I. Höflich P., Straniero O., Wheeler J.C. 1998, in the Cosmos V, Eds. N. Prantzos & S. Harissopulos, Editions Frontieres, Paris, p. 248

Fisher A., Branch D., Höflich P., Khokhlov A. 1998, ApJ 494, 47

Garcia-Senz D., Woosley S.E. 1995, ApJ 454, 895

Gerardy, C.L, Höflich P., Fesen R., & Wheeler J.C. 2001, ApJ in preparation

Harkness R. 1987, in: 13th Texas Symposium on Relativistic Astrophysics, World Scientific Publishing Co., p. 413

Hasegawa, A. 1985, Adv. Phys. 34, 1

Hatano K., Branch D., Lentz E.J., Baron E., Filippenko A.V., Garnavich P. 2000, ApJ 543L94,

Höflich P., Nomoto K., Umeda H., Wheeler J.C. 2000, ApJ 528, 590

Höflich, P., Khokhlov, A., Wheeler, J.C., Phillips, M.M., Sunzeff, N.B., Hamuy, M. 1996a, ApJ 472L, 81

Höflich, P., C. Dominik, A. Khokhlov, K. Nomoto, F.K. Thielemann, J.C. Wheeler 1996b, in: Thermonuclear Supernovae, eds. R. Canal et al., Kluwer Academic Publisher, p. 659

Höflich, P. 1995, ApJ 443, 89 [H95]

Höflich P., Khokhlov A., Wheeler J.C. 1995, ApJ 444, 211 [HKW95]

Howell A., Höflich P., Wang L., Wheeler J.C. 2001, ApJ, in press

Hoyle P., Fowler W.A. 1960, ApJ 132, 565

Iben I.J, Tutukov A.V. 1984, ApJS 54, 335

Itoh N., Mitake S., Iyetomi H., Ichimaru S. 1983, ApJ 273, 774

Kraichnan R.H., 1967, Phys. Fluids 10, 1417

Kraichnan R.H., Montgomery D. 1980, Rep. Prog. Phys. 43, 547

Müller E., Janka H.-T. 1997, A&A, 317, 140

Iwamoto, K., Brachwitz, F., Nomoto, K., Kishimoto, N., Umeda, H., Hix W.R., Thielemann F.K. 1999, ApJS 125, 439

Khokhlov A. 2001, ApJ, in press & astro-ph/0008463

Khokhlov A., Oran E.S., Wheeler J.C. 1997, ApJ, 478, 678

Khokhlov A. 1995, ApJ 449, 695

Khokhlov A. 1991, A&A 245, 114

Landau L.D., Lifshitz E.M. 1989, in: Fluid Mechanics, Vol. 6, Pergamon Press

Lentz E.J., Baron E., Branch D., Hauschildt P., Nugent P.E. 2000, ApJ 530, 966L

Limongi, M., Straniero, O., Chieffi, A. 2000, ApJS129, 625

Lisewski A. M., Hillebrandt W., Woosley, S. E., Niemeyer J., Kerstein A. R. 2000, ApJ 537, 405

Livne E. 1999, ApJ 527, 97L

Livne E. 1998, talk in workshop on SNe Ia & private communication with P. Höflich, Aspen 1998.

Livne E. 1993, ApJ 406, 17L

Mazzali P., Nomoto K., Cappellaro E., Nakamura T., Umeda H., Iwamoto K. 2001, ApJ, accepted

Metcalfe T.S., Winget D.E., Charbonneau P. 2001, ApJ, submitted

Niemeyer J. 1999, ApJ 523L, 57

Niemeyer J., Hillebrandt, W., Woosley S. E. 1996, ApJ 471, 903

Niemeyer, J., Hillebrandt, W. 1995, ApJ 452, 779

Nomoto, K. 1982, ApJ 253, 798

Nomoto, K. 1980, SSRv 25, 155

Nomoto K., Sugimoto S., & Neo S. 1976, ApSS, 39, L37

Nugent, P., Baron, E., Hauschildt, P., & Branch., D. 1997, ApJ 485, 812

Ostriker E.C., Gammie C.F, Stone J.M. 1999, ApJ 513, 259

Paczyński B. 1985, in *Cataclysmic Variables and Low-Mass X-Ray Binaries*, eds. D.Q. Lamb & J. Patterson, (Dordrecht: Reidel) p. 1

Porter D.H., Woodward P.R. 1994, ApJS, 93, 309

Porter D.H., Woodward P.R. 2000, ApJS, 127, 159

Rakavy, G.; Shaviv, G. 1968, Ap&SS 1, 347

Reinecke M., Hillebrandt W., Niemeyer J., Klein R., Gröbl A. 1999, A&A 347, 724

Rose W, Sulem P.L. 1978, Journal de Physique 39, No. 5, p. 441

Schaller G., Shaerer D., Meynet G., Maeder A. 1992, A&AS 96,269

Salaris M.; Cheffie, A. Straniero, O. 1993, ApJ, 414, 580

Stein J., Barkat Z., Wheeler J.C. 2001, ApJ, in preparation

Stone J.M., Ostriker E.C., Gammie C.F. 1998, ApJ 508, L99

Straniero, O. 1988, A&AS, 76, 157

Thielemann F.K., Nomoto K., Hashimoto M. 1996, ApJ 460, 408

Umeda, H., Nomoto, K. 1999, ApJ 513, 861

Vazquez-Semadeni E. 1991, PhD-thesis, supervised by J. Scalo, U. Texas at Austin

Whelan J., Iben I.Jr. 1973, ApJ 186, 1007

Wheeler J. C., Höflich P., Harkness R. P., Spyromilio J. 1998, ApJ 496, 908

Woosley S. E., Weaver T.A., Taam R.E. 1980, in: Type I Supernovae, ed. J.C.Wheeler, Austin, U.Texas, p.96

Woosley S.E., Weaver T.A. 1994, ApJ 423, 371

Yamaoka H., Nomoto K., Shigeyama T., & Thielemann F. 1992, ApJ 393, 55

This preprint was prepared with the AAS LATEX macros v4.0.

Table 1: Influence of the enhancement factor F of the nuclear reactions on the distance r(ignition) at which the thermonuclear runaway occurs, on the mean carbon-concentration C, and the kinetic energy at the onset of the runaway.

Factor $F$	C	r(ignition)	$E_{kin}$
200	26+-1 %	90  km	-
50	32.5~%	$86~\mathrm{km}$	-
20	35.5~%	$71~\mathrm{km}$	8.5E+45 erg
4	36.2~%	$32~\mathrm{km}$	8.2E45~erg
1	37.0~%	$27~\mathrm{km}$	6.9E45~erg

Fig. 1.— Density, carbon concentration, nuclear reaction rate and entropy (in CGS) are given for the WD with a radius of 1800 km at 3 hours before the runaway for the 2-D model, i.e. about 15 minutes after the start of the 2-D calculations. Up to this time, the changes in the chemical structures are negligible. The coordinates are given in *cm* relative to the center of the WD. The computational domain in radius and angle is 65 to 2000 km and 45° to 135°, respectively. The horizontal axis is the axis of symmetry. Note that the carbon abundance in the outer layers is 0.5, i.e. outside the color range.

Fig. 2.— Evolution of the structure during the 'mixing' phase. Carbon concentration at the inner layers of the WD as a function of time before runaway (b.r.). The coordinates are given in cm relative to the center of the WD.

Fig. 3.— Same as Fig. 2, but for the nuclear reaction rates.

Fig. 4.— Same as Fig. 2, but for the entropy. In addition, the velocity fields are given. Black, red and green vectors correspond to velocities in the ranges between 0 to 20 km/sec, 20 to 40 km/sec, and 40 to 60 km/sec, respectively.

Fig. 5.— Mass fraction and size of the region with low C  $(X(C) \le 45\%)$  as a function of time.

Fig. 6.— Carbon concentration (left) and entropy (right) at three hours (upper) and one minute (lower) before runaway. Runaway occurs when the mean entropy in the turbulent core rises to about 10.1. Note that the final size of the mixed region corresponds to the distance at with the same entropy can be found in the initial model (see text).

Fig. 7.— Final evolution of the temperature structure up to the runaway. In the lower left plot, the runaway occurs in the second red zone from the left right at the inner boundary (T=1.74<sup>9</sup> K). In addition, the velocity field is given. Black, red and green vectors correspond to velocity ranges of 0 to 50, 50 to 100, and 100 to 150 km/s, respectively.

Fig. 8.— Final evolution of the temperature structure up to the runaway for a model with the same physics as the reference model but with a smaller inner 'core' of 13.7 km instead of 65 km. For computational efficiency, the nuclear rates have been increased up to about 1 minute before the runaway. The runaway occurs in the left, upper red cell (T=5.14E9 K). The cell has a size of  $\approx 2km$  and it is at a central distance of 27km. The neighbouring red cell has a temperature of 1.06E9 K, i.e. before runaway. In addition, the velocity field is given. The longest vectors in black, red and green correspond to velocities of 50, 100, and 150 km/s, respectively. Typically, the velocities are between 30 and 60 km/sec.

Fig. 9.— Same as Fig. 8, but carbon concentration, temperature, nuclear energy generation and entropy at the runaway for the model with an inner cavity of 13.7 km. In this cell C (and O) has been depleted by the explosive nuclear burning.

Fig. 10.— Effect of the nuclear reaction rate on C-abundance and the distance at which the runaway occurs for a nuclear reaction rate increased by a factor of 4 (upper) compared to 1 (lower).

This figure "f1.gif" is available in "gif" format from:

This figure "f2.gif" is available in "gif" format from:

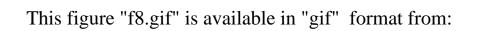
This figure "f3.gif" is available in "gif" format from:

This figure "f4.gif" is available in "gif" format from:

This figure "f5.gif" is available in "gif" format from:



This figure "f7.gif" is available in "gif" format from:



This figure "f9.gif" is available in "gif" format from:

